PHYSICAL REVIEW B VOLUME 25, NUMBER 7 1 APRIL 1982

Molecular-dynamics study of melting in two dimensions. Inverse-twelfth-power interaction

Jeremy Q. Broughton, George H. Gilmer, and John D. Weeks
Bell Laboratories, Murray Hill, New Jersey 07974
(Received 28 September 1981)

Results of a molecular-dynamics computer simulation of the solid-fluid transition in two dimensions for a system of 780 particles interacting with a purely repulsive r^{-12} pair potential are presented. The pressure as a function of density along the $T=1$ isotherm has a narrow nonmonotonic region with a symmetric loop, indicative of a weak first-order melting transition. This identification and the location of the transition is in good agreement with that obtained from an analysis of the free energies of the fluid and solid phases. Equilibration problems are found in the solid phase and the melting of a defective solid is also investigated. The behavior of the pair distribution function, angular correlation function, diffusion constant, and the defect structure uncovered by an analysis of nearest-neighbor polygons is generally consistent with a first-order mechanism. Evidence for direct fluid-solid coexistence is presented. However, a very small fluid-solid interface tension is indicated, and there is a rapid growth in the range of correlations in the fluid near freezing. The behavior of the elastic constants at melting is in fairly good agreement with the Halperin-Nelson melting criterion.

I. INTRODUCTION

Recently there has been a great deal of experimental and theoretical effort devoted to the study of the melting transition in two dimensions (2D).[1] Experimental systems studied include the melting of monolayers of rare-gas atoms on graphite,[2] electrons on He films,[3] polystyrene spheres on water,[4] and thin liquid-crystal films.[5] Furthermore the melting of a 3D crystal is often initiated by the disordering of layers of atoms adjacent to free surfaces or grain boundaries where the crystalline order is less stable than in the bulk.[6]

Early computer-simulation work on hard disks[7] and the Lennard-Jones (LJ) solid[8] suggested that 2D melting, like 3D melting, is a first-order transition, dominated by geometric packing considerations.[9] The 2D system thus seemed to offer a simpler and more easily visualized testing ground for uncovering the basic mechanisms and properties of melting that would also apply to 3D systems.

However fluctuations become more important in systems of low dimensionality and can often affect the nature of phase transitions. Long ago Peierls[10] and Landau[11] pointed out that a 2D solid does not possess the conventional long-ranged order of the 3D solid. The mean-squared displacement of a particle from its ideal lattice site will diverge as $\ln N$, where N is the number of particles, because of long-wavelength phonon fluctuations. This $\ln N$ behavior has been observed even for the small values of N possible in computer simulations.[12,13] While these fluctuations have only a very small effect on the mean-squared displacement for realistic values of N, they affect other important properties of the 2D solid such as the structure factor $S(k)$ much more strongly.[14] These effects have also been seen in computer simulations.[13,15]

It is natural to ask whether long-wavelength fluctuations could also play a role in the melting transition for some 2D solids. The first quantitative efforts along these lines were made by Kosterlitz and Thouless (KT).[16] They suggested that 2D melting could arise from the thermally driven unbinding of dislocation pairs. In the KT theory of melting the important physics occurs at long wavelengths determined by the separation of the largest dislocation pair. At the melting temperature T_m there is a continuous (conventionally called second order) transition as the separation of the largest dislocation pair tends to infinity and the solid loses its resistance to shear because of the free dislocations that result.

Halperin and Nelson[17] (HN) and Young[18] have worked out the detailed consequences of the KT mechanism. HN showed that if the dislocation unbinding mechanism of KT is correct, then at constant density the solid melts first by a continuous transition at a temperature T_m into an intermediate hexatic phase characterized by exponentially decaying positional correlations but (quasi-) long-ranged angular order. This will be discussed in more detail later. At a temperature T_2 they show that a similar mechanism involving the unbinding of disclination pairs would cause a continuous transition into the ordinary fluid, which has both exponentially decaying positional and angular correlations.

Since the theory focuses on long-wavelength properties, HN used renormalization-group methods to

make a number of specific, and in principle testable, predictions about the melting transition which should be independent of the details of the microscopic interactions. If the dislocation unbinding mechanism is correct, these predictions should be exact.

However, as HN point out, the dislocation unbinding mechanism assumed in the theory need not be correct for all (or any!) systems. A first-order transition at a temperature $T_{m'} < T_m$ could intervene before the solid becomes unstable to dislocation-pair separation and the solid could melt directly into the ordinary fluid. Chui[19] has recently developed a theory of 2D melting which predicts a first-order transition driven by the formation of grain boundaries at such a $T_{m'}$.

Indeed a first-order transition is what is suggested by the early computer-simulation data and traditional ideas about melting. The geometric packing ideas assert that the important physics for melting is occurring not at long wavelengths but at short wavelengths, e.g., those appropriate for describing the "caging" of a particle by its nearest neighbors. However in 2D we can imagine a competition between the short- and long-wavelength fluctuations leading to the melting transition. Different potentials, or different thermodynamic states, might favor one over the other.

Even if the details of the dislocation or disclination unbinding mechanisms are incorrect for some (or all) systems, one should not rule out the possibility of an intermediate hexatic phase separated from the ordinary fluid or solid by a weak first-order transition.

Stimulated by these different possibilities, there have been several recent computer-simulation studies of melting for a number of different 2D systems.[13,15,20–28] The most studied system, the LJ solid, has also produced the greatest difference of opinion. Frenkel and McTague[20] and Tobochnick and Chester[15,21] have found some evidence favoring the HN theory for states near the triple point. However, Abraham and co-workers,[22,23] Toxvaerd,[24] and van Swol, Woodcock, and Cape[25] believe their data strongly favors a conventional first-order transition. At very high densities, Tobochnick and Chester[15,21] also find evidence for a first-order transition. They point out that it is very difficult to distinguish between the properties of an ordinary two-phase region and those of the hexatic phase; for this reason they make no definite statements about the nature of the transition for the low-density LJ solid. However the constant pressure method of Abraham[22] should, in principle, avoid some of the difficulties associated with a two-phase region.

This disagreement raises the question of whether computer-simulation methods are capable of resolving basic questions about melting in 2D. Indeed there are severe problems associated with all such simulations. Most of these arise from the fact that even the longest computer-simulation run corresponds to a very short time on a laboratory scale. While equilibrium can be readily achieved in the ordinary fluid state with relatively short simulation runs it is much less likely that the same holds true for the solid near melting. This problem is particularly acute for dislocation climb, which requires vacancies or interstitials.[1,29] Yet access to all dislocation configurations is needed to provide an adequate test of the KT ideas. Further difficulties arise in attempting to describe the transition from the solid to the fluid. Achieving equilibrium in the intermediate hexatic phase, if such exists, is hampered by "critical slowing down" of the angular correlations which should occur, in principle, in the entire hexatic phase. Another complication is the possibility that the finite-system size and periodic-boundary conditions could modify the apparent nature of the phase transition.[30]

Of course if the conventional ideas about melting are correct, long-wavelength fluctuations are not important and we do not have to worry about most of these problems. A computer simulation of 2D melting should then be a relatively straightforward procedure and we can draw on the previous experience of workers studying 3D melting. However, to provide an adequate test of the KT and HN ideas, and indeed to see if any interesting behavior at all arises from the long-wavelength fluctuations, we must try to deal with the above complications.

We believe this is not an impossible task. Workers simulating phase transitions of the KT type in lattice models have been able to deal successfully with many of the problems involving critical slowing down and the influence of boundary conditions on phase transitions.[30,31] Furthermore the effects of long-wavelength fluctuations on the *positional* order in the 2D solid are observed in simulations[12,13] despite the fact that here too there is critical slowing down of the positional correlations.

Problems involving the very slow dynamics of dislocation climb and production of other defects in the solid[29] appear to us more serious, but we can check whether systems with extra vacancies or interstitials have different properties. In general, if we are aware of the likely pitfalls in straightforward simulations and make efforts to surmount them, it seems to us possible to gain useful information about the nature of the melting transition from computer simulations. In this we are aided by the fact that the HN theory[17] is a self-consistent approach which makes a number of different quantitative predictions. Some will be easier to check than others but all must hold true if the theory is correct.

This optimistic viewpoint led us to undertake a systematic study 2D melting for different systems interacting with a repulsive inverse power r^{-n} potential. There are several reasons for studying such systems. Because there is no characteristic length in the poten-

tial, inverse power systems have a useful scaling property[9,32] which allows the entire equation of state to be determined from that of a single isotherm. Thus for fixed n there can be only one kind of melting transition.

However the nature of the transition could change as n is varied. While the melting transition is generally believed to be first order for the hard-disk ($n=\infty$) system,[7] it is possible that the softer interactions occurring for small n might enhance the possibility of a continuous melting transition. The system is far from the very anharmonic hard-disk limit and geometric packing considerations may be less important. The KT picture[16] of harmonic phonons interacting with bound dislocation pairs also seems more appropriate for these soft potentials.

There have already been several simulation studies for inverse power systems in 2D. As mentioned above the hard-disk ($n=\infty$) system is generally believed to have a first-order melting transition,[7,15] though further work seems called for. At the other extreme, the $n=1$ system, studied experimentally by Grimes and Adams,[3] has been examined in computer simulations by Gann *et al.*[13] and by Morf.[27(a)] Gann *et al.* suggest that their data favor a weak first-order transition while Morf finds the behavior of the shear modulus can be explained very well using the HN theory. Very recently Kalia *et al.*,[27(b)] have studied the $n=1$ and 3 systems and have concluded that the transition in both cases is first order. McTague *et al.*[28] have begun Monte Carlo simulations on the $n=6$ system and find some features in accord with the HN theory, but because of very sluggish behavior near the transition they can reach no definite conclusions. Finally, van Swol *et al.*[25] have studied the $n=12$ system and analyzed their data under the assumption that there is a first-order transition. Although they treated a very large system, the short runs they made were probably not sufficient to permit equilibration in the phase-transition region.

In this paper we report results of a MD simulation of the $n=12$ system with particular attention paid to the region near the melting transition. The second paper in this series will describe a truncated version of the $n=3$ system and discuss the changes arising from "softening" the interaction potential as well as the general trends found in the simulations done to date.

After describing in Sec. II some details of the molecular dynamics (MD) method and the systems studied, we examine in Sec. III the equation of state near the phase-transition region. These data suggest a conventional first-order transition. This identification is strengthened in Sec. IV by a calculation of the free energies of the solid and fluid phases which gives a first-order transition whose location is in good agreement with that found in Sec. III. After a discussion of trajectory plots in Sec. V, we report in Sec. VI an attempt to observe two-phase coexistence directly.

Section VII discusses the defect properties of the solid and fluid phases uncovered by the nearest-neighbor analysis using the Voronoi polyhedra. Sections VIII and IX contain discussions of positional and angular correlation functions, Sec. X velocity autocorrelation functions and diffusion constants, and Sec. XI the behavior of the elastic constants near the melting transition. Concluding remarks are found in Sec. XII.

II. GENERAL CONSIDERATIONS

A. Systems studied

We performed MD calculations[33] for a system with 780 (26×30) particles of mass m interacting with the pair potential

$$u(r)=\epsilon(\sigma/r)^{12}\ , \tag{2.1}$$

truncated at $r=2.5\sigma$. Here σ has dimensions of length and ϵ energy. Assuming periodic-boundary conditions we confine the particles to a rectangular (very nearly square) unit cell whose ratio of height to width is $(26/30)(2/\sqrt{3})=1.000\,74$; this cell accommodates a section of a perfect unstrained hexagonal lattice. We generally used a time step $\Delta t=0.005\times(\epsilon/m\sigma^2)^{-1/2}$. (In the following we use reduced units where $\sigma=\epsilon=m=1$.) A typical (Einstein) vibrational period in the solid near the melting density is $(80-100)\Delta t$. To check whether the boundary conditions and fixed particle number N artificially stabilized the solid phase we also studied the melting of a solid with a single vacancy, i.e., 779 particles in the same unit cell. (As might be expected for this relatively "hard" system, the energy of a vacancy at $T=0$ is much less than that of an interstitial.)

We studied the melting and freezing transitions along the $T=1$ isotherm. The scaling property of inverse power potentials discussed in Appendix A allows us to determine from this data properties along any other isotherm. We traversed the isotherm near the phase-transition region in both directions. That is, we started from a high-density perfect solid or solid with a single vacancy and considered states with successively lower density (referred to as the S or S_V traverse.) Starting from a state in the ordinary fluid region, we also considered states of successively higher density (referred to as the F traverse). The density was varied by a uniform rescaling of the final position coordinates from the previous state of that traverse and velocities were rescaled and sometimes randomized during an initial equilibration run until a stable temperature $T=1$ (determined by the average kinetic energy) was achieved. If necessary, additional very small and infrequent rescalings of the velocity were made to maintain an essentially constant temperature.[33]

B. Run times

Away from the phase-transition region only relatively short runs were required to achieve consistent results. We generally made an equilibration run of $12\,000\Delta t$ before taking statistics over the next $12\,000\Delta t$. Much shorter runs gave stable thermodynamic properties but some structural properties very sensitive to long-wavelength fluctuations such as the angular correlation function required the longer equilibration period.

In the vicinity of the melting transition ($0.97 \lesssim \rho \lesssim 1.02$) much longer runs were made, particularly in the middle of this region where we attempted to distinguish between hexatic and two-phase behavior. A typical equilibration run time was $48\,000\Delta t$ with statistics taken over the next $24\,000\Delta t$ and even then, as discussed in detail later, we observed differences in results from the F and S traverse. (The S_V traverse produces results in close agreement with those from the F traverse.)

III. EQUATION OF STATE

In this section we examine the behavior of the pressure along the $T=1$ isotherm to try to determine the nature of the phase transition. There are some practical advantages in analyzing thermodynamic functions along an isotherm rather than an isochore since distinctions between behavior expected for first- and higher-order transitions are more apparent. In an infinite system the constant pressure in the two-phase region along an isotherm implies a very large change in slope of the P-ρ curve. This change is less noticeable along an isochore and is more easily confused with the behavior expected for a continuous transition.

These advantages persist for finite systems. Mayer and Wood[34] have analyzed the behavior to be expected along an isotherm at a first-order transition for a finite system at equilibrium with periodic-boundary conditions. They find there should be a symmetric loop in the P-ρ curve in the two-phase region. Because of the nonzero interface tension between the fluid and solid phases, the finite system initially overshoots the infinite system's coexistence pressure in the F traverse to avoid forming a "droplet" of the solid phase. Similar arguments apply to the S traverse. The size of the overshoot is an increasing function of $\tau/N^{1/2}$ where τ is the interface tension, and it vanishes in the limit $N \to \infty$. There can be regions in the loop where $(\partial P/\partial\rho)_T < 0$, which of course violates stability for an infinite system. Such a region in the P-ρ plane seems very hard to explain except by assuming a nonzero interface tension between two phases. The analysis of Mayer and Wood[34] ignores fluctuations and hence probably overestimates the size of the overshoot and is by no means rigorous, but does give a reasonable first approximation to the behavior that might be expected at a classical first-order transition for a finite system.

Figure 1 shows the pressure as a function of density near the phase-transition region. The crosses denote the S traverse and the squares the reverse F traverse. The F traverse started at a density $\rho=0.970$ (obtained by densification of a $\rho=0.930$ fluid) which we identified by several criteria to be discussed later as a stable ordinary fluid state. We do not observe large fluctuations in the angular order or other properties at this density.

We note that the F traverse agrees well with the S data until about $\rho=0.985$ where noticeably different behavior is seen. Both curves have loops which we would be tempted to associate with a first-order transition. However since the loops do not coincide the system must not be in equilibrium in this region for one (or both!) of the traverses.

We believe the major equilibration problem is associated with the S traverse. The boundary conditions stabilize the perfect solid and inhibit the formation of interstitials and vacancies, which at fixed N must form in pairs. Although these defects are not important at low temperature, near melting they aid in dislocation climb[29] and may also serve as nucleation centers for "droplets" of the fluid phase. The very large loop and nearly vertical jump on the S traverse are consistent with the melting of a metastable solid with an artifically large kinetic barrier to melting, possibly resulting from the problems with forming interstitials and vacancies. The nearly vertical jump in P occurs at a density in the range $0.993 < \rho < 0.995$; and at the same time the diffusion constant increased

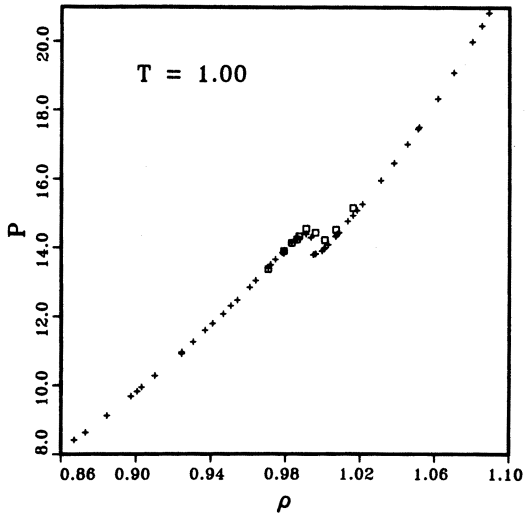

FIG. 1. $T=1$ pressure vs density isotherm. Squares represent the F traverse, crosses represent the S traverse.

dramatically.

In the fluid phase there is more rapid diffusion and the system is much more likely to be in equilibrium. Indeed the F and S traverse give the same result here. As we argue in detail later the fluid near freezing is by 3D standards very well ordered with large patches of local crystalline-like order. This suggests there is a small fluid-solid interface tension and little nucleation barrier to freezing. The small and symmetric loop we find in the F traverse is in accord with these expectations (and corresponds to case C discussed by Mayer and Wood[34]).

In the solid phase the F and S pressures do not coincide even at the highest density. Inspection of the configurations (discussed later) shows that the fluid had crystallized into a defective solid misoriented with respect to the boundaries. This misoriented state seems stable indefinitely, again showing the problems in equilibrating defects in the solid near melting. It seems likely that an excessive number of defects are frozen in by this process and the true equilibrium pressure in the solid lies between the S and F values.

To check the effects of defects on the melting of the solid phase we show in Fig. 2 the F traverse and the S_V traverse together with the S data for the solid. The melting of the solid with a single vacancy gives a much smaller loop than did the S traverse and now produces very good agreement with the F traverse. This is strong evidence that the equilibration problem indeed is associated with the boundary stabilized perfect solid. Stillinger and Weber[26] also found reproducible freezing and melting behavior for the 2D

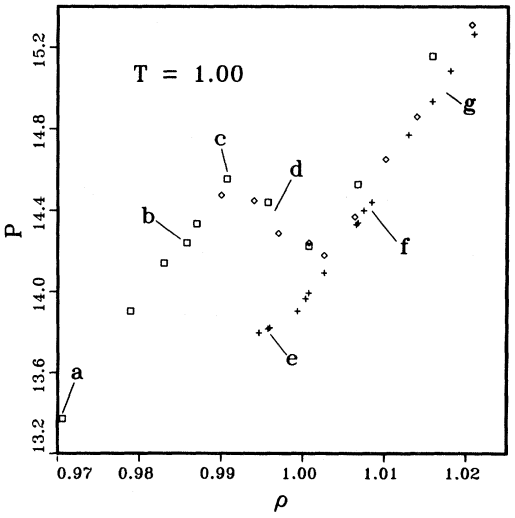

FIG. 2. $T=1$ hysteresis region. Squares represent the F traverse, crosses represent the S traverse and diamonds represent the S_V traverse. Letters $a-g$ locate states whose properties will be discussed later.

Gaussian core model if a slightly defective solid was used.

If the S_V and F loops are indeed in equilibrium, the theory of Mayer and Wood[34] justifies an "equal areas" construction. This analysis suggests that there is a conventional first-order transition with a pressure at melting of about $P_m=14.34$ and freezing density $\rho_l=0.987$ and melting density $\rho_s=1.006$.[35] Errors in these densities of about ± 0.001 arise from problems in graphically determining equal areas using the data in Fig. 2. This 2% change in density on melting should be compared to the 4.8% change found in 3D.[31]

IV. FREE-ENERGY CALCULATION

We can also locate the phase-transition region by a calculation of the free energies in the two phases. To do this we continue the equation of state in the fluid phase to very low densities where the virial expansion is accurate. The free energy can then be calculated relative to that of the ideal gas. In the solid phase we calculate the free energy relative to that of the harmonic solid, whose free energy can be calculated analytically using lattice dynamics.[36] We assume that corrections to the harmonic energy at constant density can be expressed as a perturbation expansion with T^2, T^3, ... terms. In scaling form this implies an expansion using terms ρ_*^{-6}, ρ_*^{-12}, . . . , where ρ_* is the scaled density-temperature variable defined in Appendix A.

In the fluid phase we have calculated the equation of state for 60 points varying from $\rho=0.050$ to 0.991 along the $T=1$ isotherm. We fit the data to a polynomial of eight terms, in which the first two are the exact second and third virial coefficients for this potential,

$$\frac{\beta\Delta P}{\rho}=1.773\,06\rho_*+2.362\,41\rho_*^2+1.798\,198\rho_*^3-5.648\,177\rho_*^4+78.657\,12\rho_*^5-197.572\,41\rho_*^6+212.374\,17\rho_*^7-79.574\,56\rho_*^8 \quad . \tag{4.1}$$

Here ΔP is the excess pressure over the ideal gas. The rms error was 2.4×10^{-2}. Van Swol *et al.*[25] have used a similar expression which is in good agreement with Eq. (4.1) except near the phase-transition region.

The chemical potential is then given by integration from $\rho=0$ of the thermodynamic expression

$$\left(\frac{\partial\Delta\mu}{\partial\rho}\right)_\beta=\rho^{-1}\left(\frac{\partial\Delta P}{\partial\rho}\right)_\beta \quad . \tag{4.2}$$

Thus we find

$$\beta\Delta\mu=3.546\,12\rho_*+3.543\,61\rho_*^2+2.397\,598\rho_*^3-7.060\,217\rho_*^4+94.388\,54\rho_*^5-230.501\,14\rho_*^6+242.713\,3\rho_*^7-89.521\,38\rho_*^8 \quad . \tag{4.3}$$

In the solid phase to connect with the harmonic solid we studied 30 points along the $\rho = 1.0$ isochore from $T = 0.01$ to 0.996. We found that this data and the rest of our solid phase data on the $T = 1$ isotherm could be accurately fit with an rms error of 1.6×10^{-3} using only two terms in the perturbation expansion discussed above. Using scaling the pressure can then be expressed as

$$\frac{\beta \Delta P}{\rho} = \frac{\beta \Delta P_H}{\rho} - 1.259\,46\rho_*^{-6} + 0.597\,61\rho_*^{-12} \quad . \tag{4.4}$$

In Appendix A we give expressions for $\beta \Delta P_H/\rho$. [These anharmonic corrections in Eq. (4.4) were determined using pressure data for the perfect 780 particle solid which might have artificially low pressure because of the difficulty of defect formation. Errors induced by this assumption will be discussed later.] Again we find good agreement with the similar expression of van Swol *et al.*[25] Eq. (4.4) implies that the anharmonic corrections reduce the potential energy of the solid near melting by about 5% below that of the harmonic solid. As the exponent n gets larger this reduction must be even more dramatic—there is no potential energy at all in the hard, anharmonic, $n \to \infty$ limit.

Integrating the difference $\Delta P - \Delta P_H$ down from $\rho = \infty$ where the difference vanishes, we find from Eq. (4.2)

$$\beta \Delta \mu - \beta \Delta \mu_H = -1.049\,55\rho_*^{-6} + 0.547\,81\rho_*^{-12} \quad . \tag{4.5}$$

Again $\beta \Delta \mu_H$, which requires a lattice dynamics calculation, is given in Appendix A.

Using these we can determine the coexistence pressure and densities by requiring equality of pressure and chemical potential in the two phases, or equivalently, by using the Maxwell double tangent construction. Figure 3 shows this construction. Note the very small vertical scale. The slopes of the free-energy curves are very nearly equal and it is only by removing the dominant term linear in ρ^{-1} that any curvature at all can be seen on the scale of the graph.

The coexistence densities $\rho_l = 0.991$ and $\rho_s = 1.011$ and pressure $P = 14.64$ so determined are in fairly good agreement with those found before using the equal areas construction on the loop from the F traverse. However the coexistence pressure, $P = 14.64$ so determined is slightly higher than that of point c in Fig. 2 which is the highest pressure in the hysteresis region. We note that the free-energy calculations of Barker *et al.*,[23] for the 2D LJ system also gave a coexistence pressure higher than that contained in the hysteresis region determined from Abraham's MC calculations.[22] We discuss below a possible reason for this behavior.

Since the slopes are so nearly equal it is clear that we must have very accurate data to obtain accurate coexistence densities and pressure. In the 780 particle solid near melting we have suggested there may be a systematic underestimation of the pressure because of the difficulty of defect formation. This might be expected to cause a non-negligible error in the coexistence properties. In Appendix B we give an analysis of the sensitivity of the coexistence properties to small variations (due to systematic errors) in the pressure. We find the situation is not as bad as it might seem, since errors in the pressure are partially canceled by compensating errors in the chemical potential.

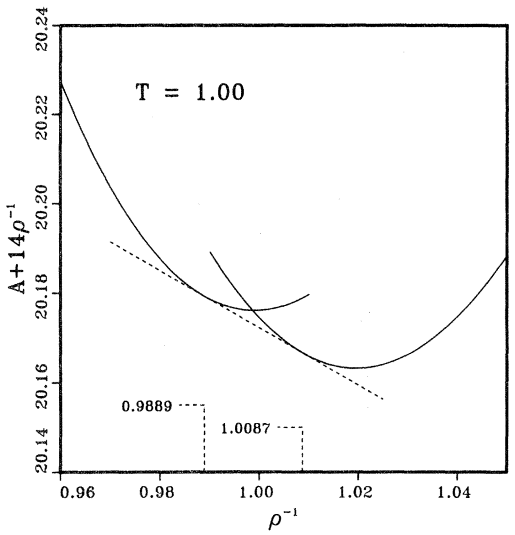

FIG. 3. Double tangent construction.

As an example let us recalculate the pressure in the solid phase using data near the melting transition taken from the system with a single vacancy. The pressure of the vacancy system differs from the perfect system at the same density by about 0.05 near melting and we believe this is likely to be closer to the (unknown) exact result.

Since at very high densities the perfect system must be more stable, we kept the harmonic terms in Eq. (4.4) unchanged and refit the anharmonic coefficients to give the vacancy system pressure near melting. Instead of Eq. (4.4) we now find

$$\frac{\beta \Delta P^{(V)}}{\rho} = \frac{\beta \Delta P_H}{\rho} - 1.240\,44\rho_*^{-6} + 0.646\,63\rho_*^{-12} \tag{4.6}$$

with a similar expression for $\beta \Delta \mu^{(V)}$. Using the same fluid data as before and this new solid data we now find coexistence at $\rho_l = 0.986$ and $\rho_s = 1.005$ with $P = 14.29$. These values now agree very well with those given by the equal areas construction and represent our best estimates.

The change in molar entropy on melting can be computed from the formula,[37] valid for all inverse

power potentials with $n > 2$,

$$\Delta s = \frac{\Delta\rho}{\rho_l}\left[1+\frac{2}{n}\right]\left[\frac{\beta P}{\rho_s}\right], \tag{4.7}$$

where $(\beta P/\rho_s)$ is the compressibility factor at melting and $\Delta\rho/\rho_l$ is the fractional change in density. Using the coexistence data above for the vacancy system we find $\Delta s = 0.32$, whereas the perfect solid data give $\Delta s = 0.34$. It is interesting to note this value agrees closely with that obtained by Stillinger and Weber[26] from the superficially very different Gaussian core model.

In the following sections we examine various structural and dynamic properties of the system near the phase transition and find results generally consistent with the above thermodynamic results, though equilibration problems and effects of finite system size show up more clearly here.

V. PARTICLE TRAJECTORIES

In order to obtain a feeling for the amount of diffusion and particle exchange going on during a MD run it is convenient to make a "trajectory plot." This plot connects by straight lines the positions of each particle at equal time intervals ΔT for m intervals during a molecular dynamics run. Usually we took $\Delta T = 600\Delta t$ and $m = 10$. Thus we have a record of particle positions over many vibrational periods. In the fluid phase there is considerable particle diffusion and the plots appear quite disordered. In the stable solid phase there is little diffusion and a well-ordered structure is found. We note a very good correlation with the amount of disorder shown by the trajectory plots and the defect fractions and other meaures of disorder discussed below.

In the intermediate region, areas of order and disorder are found and it seems natural to identify them with solid and fluid regions. However this identification by itself is ambiguous and cannot be convincingly distinguished from the behavior that might be expected in an intermediate hexatic phase because of critical fluctuations. Further, as stressed by Tobochnick and Chester,[15] the amount of apparent disorder varies with the time interval and the number of points m considered.

While it is very likely true that this behavior can be understood (assuming a first-order transition) as the wandering of "droplets" of one phase in the other it may take a very long time for these droplets formed by nucleation to aggregate and form a macroscopic region of one phase in the other. If the interface tension is small there will be large fluctuations at the boundaries of the droplet as well as a slower overall diffusion of the center of mass of the droplet and thermal fluctuations may even cause the droplet to break apart. These effects must all be carefully analyzed to distinguish between droplet fluctuations and critical fluctuations. A reasonable procedure would be to take trajectories over a time long compared to diffusion times in the fluid, but not so long that the (presumably much slower) motion of the droplet as a whole could confuse the interpretation.

Rather than attempt this procedure for an arbitrary fluid-solid configuration, we show in the next section that by setting up in advance well-defined regions of fluid and solid we can observe rather stable fluid-solid coexistence at precisely the pressure and densities found before from thermodynamic arguments.

VI. DIRECT OBSERVATION OF TWO-PHASE COEXISTENCE

To examine the stability of fluid-solid coexistence, we placed two equilibrated solid and fluid systems of the appropriate density together and followed the progress of the composite 2×780 particle system. That is, we considered a rectangular unit cell containing 1560 particles. The length was about twice the width and consistent with an overall density $\rho = 0.999$ approximately in the middle of the two-phase region as determined in Secs. III and IV. The initial coordinates of 780 particles in an essentially square slab in the middle of the box were taken from those of an equilibrated solid at its melting density. These particles were held fixed during an initial equilibration run while the remaining 780 particles, whose initial coordinates were chosen from the equilibrated fluid state, accommodated themselves at $T = 1$ to the static solid. The velocities for all particles were then chosen at random from the appropriate Boltzmann distribution at $T = 1$ and an ordinary MD run was made with all particles free to move.

We found this phase-separated state was rather stable. The regions of "fluid" and "solid" indicated by the trajectory plots in Fig. 4 corresponded to those created by our initial starting configuration for run times of at least $36\,000\Delta t$ and a stable pressure $P = 14.4$ was maintained. However, the boundaries between the phases are "rough" and would be expected to have transverse fluctuations proportional to the square root of their length. Furthermore, we have not stabilized the absolute locations of the fluid or solid slabs by boundary conditions at the sides of the box.

Thus it is perhaps not surprising that eventually fluctuations appeared to change our initial slab locations. After an elapsed time of $36\,000\Delta t$ the disordered regions appeared to coalesce in the center as shown in Fig. 5. This was accompanied by a slight rise in the pressure. After an additional $12\,000\Delta t$ times the regions of fluid and solid appeared to reverse themselves, as shown in Fig. 6, and the pres-

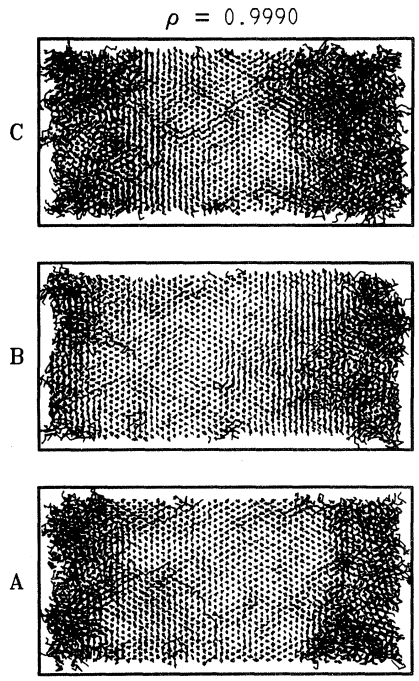

FIG. 4. Trajectory plots of two-phase coexistence. (a) represents 1–6000Δt, (b) represents 18 001–24 000Δt, (c) represents 30 001–36 000Δt.

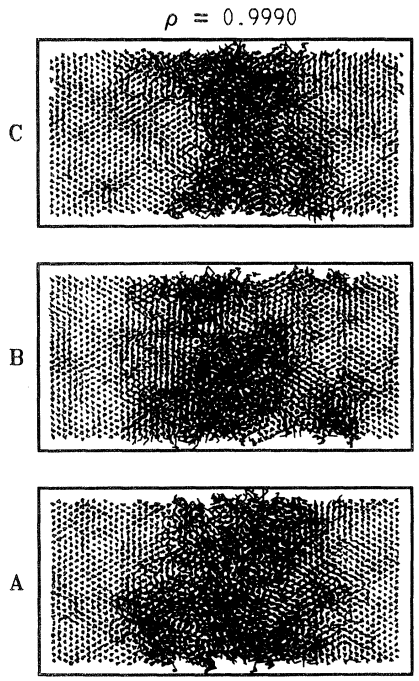

FIG. 6. Trajectory plots of two-phase coexistence. This series folows on from Fig. 5. Each plot represents an elapsed time of 6000Δt. (a)–(c) follow on contiguously from one another and represent the period 48 001–66 000Δt.

sure restabilized at a value 14.4 consistent with two-phase coexistence.

This behavior could be interpreted as arising from critical fluctuations at a continuous phase transition. In this case there is no interface tension between the "fluid" and "solid" slabs at the appropriate critical density and fluctuations would be expected to destroy the initial configuration we set up. However, we believe the behavior we observed is better interpreted as that arising from a two-phase region with a small but nonzero interface tension between the phases. After the destruction of the initial slabs the system eventually returned to a slablike arrangement favored by surface tension arguments, and seemed to maintain essentially the same fraction of solid and fluid that would be appropriate for two-phase coexistence. Furthermore, the solid phase maintained its orientation with respect to the boundaries. However, it is clear that this evidence is somewhat ambiguous and provides incontrovertible support for neither possibility. It would be interesting to repeat this experiment using a longer rectangle where the transverse fluctuations in the boundaries could not so easily bring the disordered regions together.

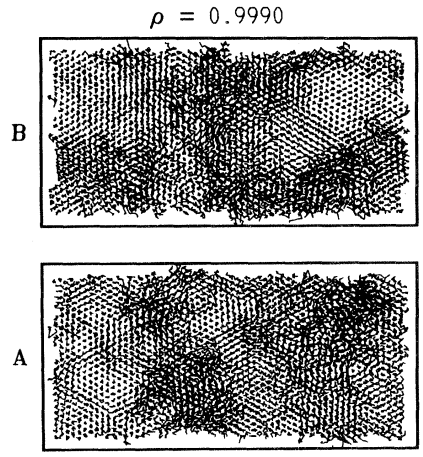

FIG. 5. Trajectory plots of two-phase coexistence. (a) represents 36 001–42 000Δt and (b) represents 42 001–48 000Δt.

VII. DEFECT PROPERTIES

As was pointed out by McTague *et al.*,[28] an analysis of the coordination numbers of each atom using the Wigner-Seitz or Voronoi construction gives a very useful characterization of the defect structure of a 2D system. In a given configuration each particle is enclosed by a convex polygon having m sides

defined as the set of points closer to particle i than to any other particle. Pairs of particles whose polygons share a common side are defined as "nearest neighbors"; hence atom i has m_i neighbors. It is a remarkable property of a 2D system that the average coordination number defined in this manner is 6, regardless of the state of disorder.[38]

For states in the dense fluid phase near freezing and in the solid this definition of nearest neighbors is in good agreement with the traditional method of counting the number of particles within a certain cutoff radius r_c [approximately equal to the first minimum in the radial distribution function $g(r)$] around a given particle. If we choose r_c to be $1.37a_0$, i.e., midway between nearest and next-nearest lattice positions, we find the average number of m-coordinated atoms determined by this method differs generally by less than one percent from that given by the Voronoi analysis.

In a perfect solid each atom has six neighbors. A particle with any other coordination represents a disclination.[28] A dislocation can be thought of as a closely bound disclination pair[17]; thus a 5-7 pair constitutes a dislocation whose Burger's vector is prependicular to the pair axis. In the solid phase only bound dislocation pairs can occur; these usually show up as 5-7, 7-5 quadrupoles with opposite Burger's vectors, though dislocation triplets with zero net Burgers's vector are also found. Defects such as interstitials and vacancies also produce their own characteristic patterns, or can be thought of as special cases of dislocation pairs. Finally grain boundaries are characterized by closed loops of 5-7 pairs.[28] Weber and Stillinger[26] have given a more complete discussion and examples of the characteristic defect patterns.

In Fig. 7 we give the Voroni analysis[39] of a typical configuration at state f in Fig. 2 of the solid phase very near ($\rho = 1.008$) the melting density. We notice only a few clusters of tightly bound dislocation pairs. Neither in this or any other stable solid configuration that we have examined have we found any dislocation pairs separated by more than two lattice constants. The same statement holds true for the imperfect solid with a vacancy, where one might have expected dislocation climb to be aided by the vacancy. The individual closely bound 5-7, 7-5 quadrupoles are very short-lived, and can annihilate and reform in a time that is less than $5\Delta t$.

In the pure fluid very near freezing at a density of 0.986 (state b in Fig. 2) we see in Fig. 8 a significant increase in the overall disorder as indicated by the large number of five- and seven-coordinated atoms. In addition to the quadrupoles we see some separated "dislocation pairs" and even some individual "disclinations." However there are surprisingly large patches of six-fold order in various orientations separated by "grain boundaries," which of course

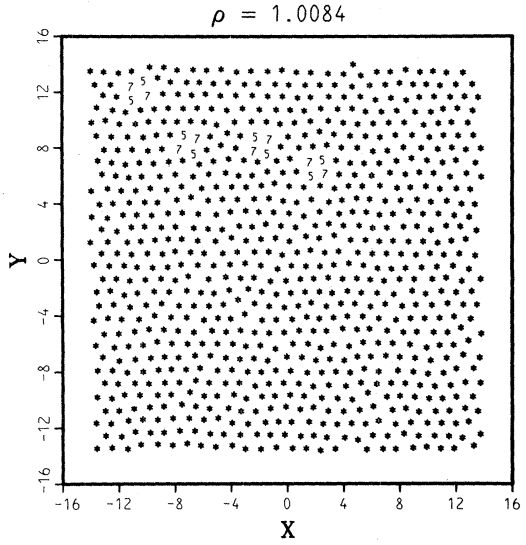

FIG. 7. Voronoi analysis of an instantaneous equilibrium configuration at $\rho = 1.008$ (state f). Asterisks represent six-coordinated atoms.

fluctuate as the simulation proceeds. These results seem in accord with the physical picture used by Chui[19] in his grain-boundary theory of melting.

Since the average coordination number in the fluid (6) is consistent with the most efficient global (crystalline) packing, this overall rather ordered structure is easy to understand. As the density is increased, packing considerations force larger local regions of

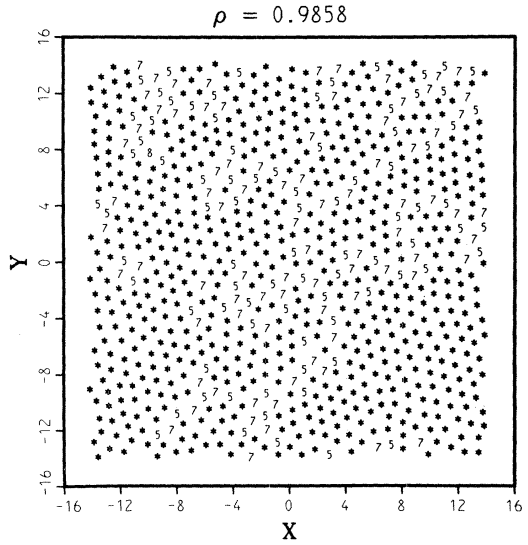

FIG. 8. Voronoi analysis of an instantaneous equilibrium configuration at $\rho = 0.986$ (state b). Asterisks represent six-coordinated atoms.

essentially perfect sixfold order. In the fluid state these different regions are misoriented and uncorrelated with each other and fluctuate sufficiently that the time averaged structure is a disordered fluid. This picture suggests that a microcrystallite model of the dense 2D fluid is much more likely to be useful than is the case in 3D and helps rationalize the large correlation length in the 2D fluid discussed in the next sections.

VIII. POSITIONAL CORRELATIONS

Figures 9 and 10 give the radial distribution functions at the five states *g*, *f*, *d*, *b*, and *a* shown in Fig. 2 in the phase-transition region. There is considerable change in these functions as the density is reduced from that of the solid to the fluid. Particularly instructive is the behavior of the third peak. In the solid phase it is higher than the second peak and has a shoulder, consistent with the hexagonal lattice structure. At states *d*, *b* and *a* in the two-phase and fluid regions the third peak is lower than the second as is usual in a fluid. However the fluid at state *b* appears very ordered when compared to typical 3D fluids. The height of the first peak and the persistence of oscillations at rather large *r* shows the extensive positional order that characterizes the dense 2D fluid. We estimate from the exponential decay of $g(r)$ in state *b* a positional correlation length $\xi = 3.1$ which compares to a value near unity for a typical dense 3D fluid near freezing.

In the two-phase region at state *d*, $g(r)$ has even more persistent oscillations but is similar to that of the fluid. Apparently the disorder and fluctuations in this region are sufficient to obscure the characteristics of the solid distribution function which might be expected from a linear combination of pure fluid and solid functions. Since the solid has only quasi-long-ranged order this is perhaps not surprising. Some evidence suggesting the presence of solid order in the two-phase region shows up in the angular correlation function $G_6(r)$ discussed below and from direct observation of the configurations.

We give in Figs. 11 and 12 the structure factor

$$S(q) = 1 + \rho \int [g(r) - 1] e^{i \vec{q} \cdot \vec{r}} \, d\vec{r} \qquad (8.1)$$

for states *a* and *b* in the stable fluid region. Hansen and Verlet[40] found that the height of the first peak in $S(q)$ varied by only a few percent for many 3D fluids at freezing and it will be interesting to see if this holds true for 2D systems. $S(q)$ also plays an essential role in the theory of freezing of Ramakrishnan and Yussouff,[41] and their prediction for the height of the first peak of $S(q)$ at freezing is in good qualitative agreement with that found in Fig. 12. Note the rapid growth of the height of the first peak in $S(q)$

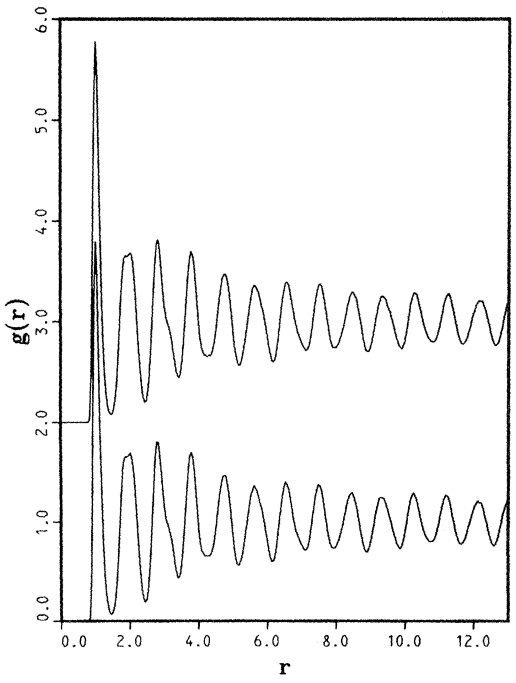

FIG. 9. Radial distribution function at $\rho = 1.016$ (state *g*) and 1.008 (state *f*). The latter curve is displaced upward for clarity.

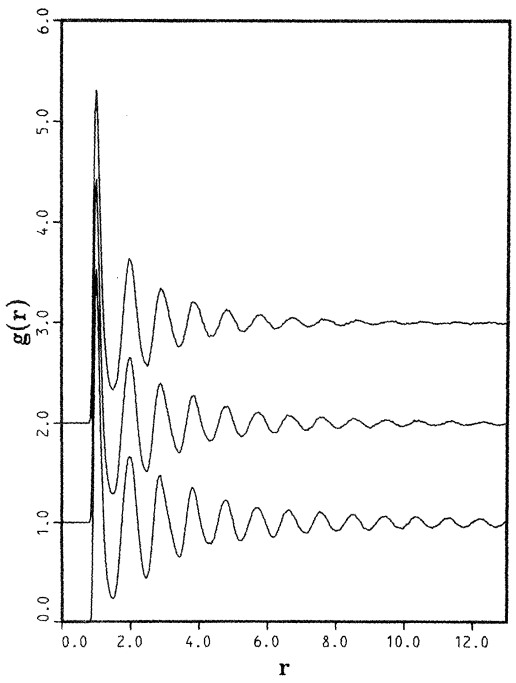

FIG. 10. Radial distribution function at $\rho = 0.993$ (near state *d*), $\rho = 0.986$ (state *b*), and $\rho = 0.971$ (state *a*). The latter curves are displaced upward for clarity.

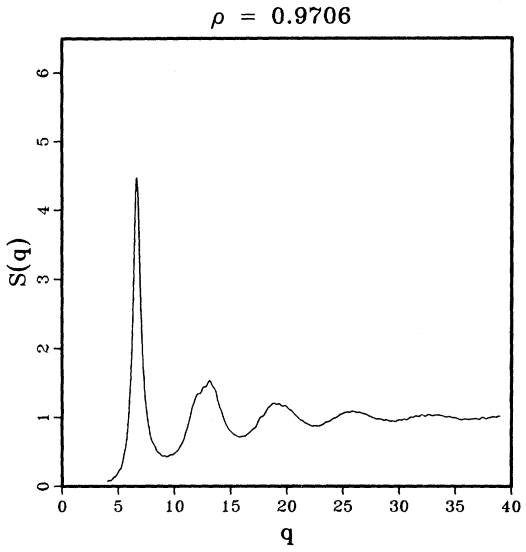

FIG. 11. Structure factor at $\rho=0.971$ (state a).

and the development of a split second peak as the density is changed from $\rho=0.971$ (state a) to 0.986 (state b). The splitting becomes even more pronounced as the density is further increased. The split peak maxima occur at the second- and third-neighbor spacing of the reciprocal hexagonal lattice. Thus there is a rapid increase in the range of correlations in the dense 2D fluid near freezing. This again shows that in two dimensions a dense fluid has more order than conventional wisdom based upon experience in three dimensions would at first suggest. It is interesting that the Fourier transform reveals greater structural order than is apparent in the $g(r)$ curve of Fig. 10. This also suggests that the correlation lengths we estimated using $g(r)$ may underestimate the actual range of correlations in the fluid.

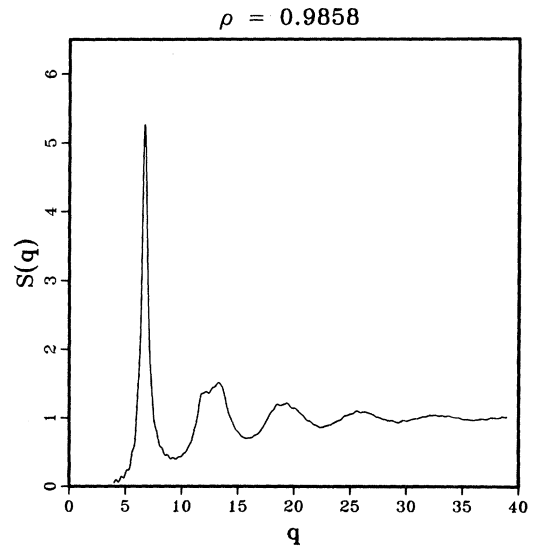

FIG. 12. Structure factor at $\rho=0.986$ (state b).

IX. LOCAL ORDER AND ANGULAR CORRELATIONS

As a measure of the local order we associate with each particle i at its instantaneous position $\vec{r}_i$ the quantity n_i defined as the number of particles ("neighbors") found within a radius $r_c=1.37a_0$ of particle i (as discussed before this is essentially identical to that given by a Voronoi analysis). In analogy to the definition of the microscopic particle density

$$\hat{\rho}(\vec{r})=\sum_{i=1}^{N}\delta(\vec{r}-\vec{r}_i) \ , \tag{9.1}$$

where $\langle\hat{\rho}(\vec{r})\rangle=\rho$ we define the microscopic density of m—coordinated atoms as

$$\hat{\rho}_m(\vec{r})=\sum_{i=1}^{N}\delta(\vec{r}-\vec{r}_i)\delta_{m,n_i} \ . \tag{9.2}$$

Then F_m, the average fraction of particles with m neighbors, is given by

$$\langle\hat{\rho}(\vec{r})\rangle F_m=\langle\hat{\rho}_m(\vec{r})\rangle \tag{9.3}$$

or

$$F_m=\rho^{-1}\langle\hat{\rho}_m(\vec{r})\rangle \ . \tag{9.4}$$

Since every atom that is not six coordinated can be thought of as part of some defect, the defect fraction $F_D=1-F_6$ gives an overall measure of the disorder in the system. If there is a continuous melting transition F_D would be expected to vary smoothly across the transition. In Fig. 13 we plot F_6 along the $T=1$ isotherm. We note a significant decrease in F_6 in the transition region, $0.986\lesssim\rho\lesssim1.006$. This rapid change is consistent with a first-order melting transition between states with very different defect structures. The fluctuations in F_6 are much greater in the two-phase region than on either side.

To measure the angular order we associate with each particle i a complex order parameter[42]

$$\psi_i=\frac{1}{n_i}\sum_{j=1}^{n_i}e^{6i\theta_{ij}} \ , \tag{9.5}$$

where θ_{ij} is the angle of the line or "bond" joining neighboring particles i and j relative to some fixed axis. In a grain with perfect crystalline order $|\psi_i|=1$ but grains with different orientations will have different phase factors. To compare angular order in different regions we consider pair correlations involving the ψ_i. Since ψ_i itself is defined using pairs of particles, these involve four-particle correlations.

As in Eq. (9.2) we define a microscopic order-

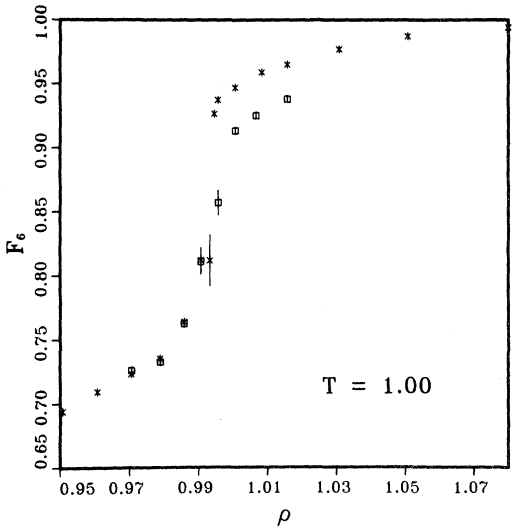

FIG. 13. Fraction of six-coordinated atoms along $T=1$ isotherm as a function of density. Asterisks represent the S traverse. Squares represent the F traverse. Vertical lines represent error limits.

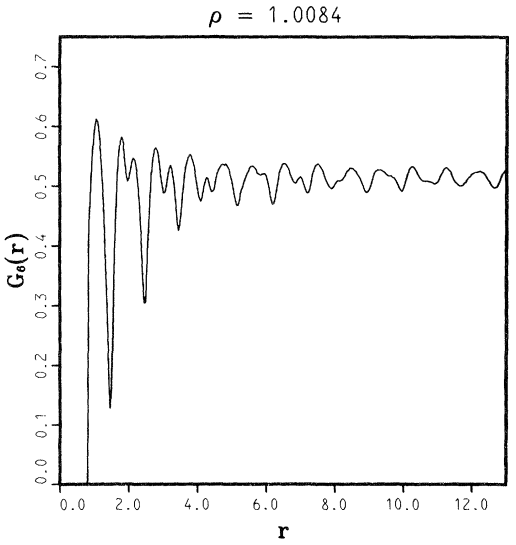

FIG. 14. Angular correlation function at $\rho=1.008$ (state f).

parameter density

$$\hat{\psi}_6(\vec{r}) = \sum_{i=1}^{N} \delta(\vec{r} - \vec{r}_i)\psi_i \ . \tag{9.6}$$

The distinction between the ordinary and hexatic fluid then shows up in the angular correlation function, $G_6(r)$, defined as

$$\langle \hat{\rho}(\vec{r}_1)\hat{\rho}(\vec{r}_2)\rangle G_6(\vec{r}_1, \vec{r}_2) = \langle \hat{\psi}_6(\vec{r}_1)\hat{\psi}_6(\vec{r}_2)\rangle \ . \tag{9.7}$$

In the (ordinary or hexatic) fluid G_6 is a function of $r_{12}=|\vec{r}_1-\vec{r}_2|$ and in the solid we consider the angle averaged quantity. Clearly $G_6(r)\leq 1$. In the solid $G_6(r)$ will reach a finite value as $r\rightarrow\infty$ indicating long-ranged angular order. The HN theory[17] predicts that $G_6(r)$ should decay to zero in the hexatic phase as $r^{-\eta}$ with $\eta\leq 0.25$, while it decays exponentially in the ordinary fluid state.

In Fig. 14 we show $G_6(r)$ for state f in the solid phase. Long-ranged angular order is clearly seen. The various oscillations in G_6 are meaningful and give information about detailed positional correlations in the hexagonal lattice. Much of this information is lost in $g(r)$, because all pairs are assigned equal weight in the average, without regard to their orientation.

Figure 15 shows $G_6(r)$ at state a ($\rho=0.971$) in the stable fluid region. We find that $G_6(r)$ tends rapidly to zero and the result is well fit by an exponential with a correlation length $\xi=2.5\sigma$. Figure 16 shows $G_6(r)$ at state b ($\rho=0.986$) which we have identified as a stable fluid at freezing; the decay is much slower and there is a nonzero tail even at $r=13.0$. The correlation length is sufficiently long that finite-size effects on $G_6(r)$ may be significant. A larger system size seems necessary to establish conclusively that $G_6(r)$ will eventually decay to zero as it should for a pure (ordinary or hexatic) fluid state and to provide definitive evidence for exponential versus algebraic decay. As we have noted before the fluid at this density is very well ordered with large "grains" with rather well-defined angular order. In order for G_6 to decay to zero we must have a system size large enough to contain several such grains and perform runs of sufficient length to permit averaging over

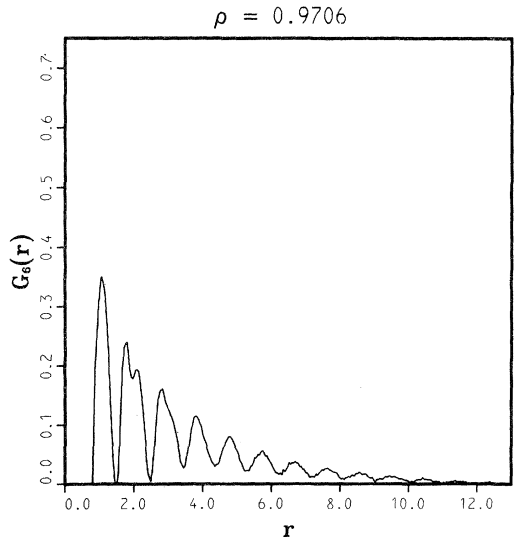

FIG. 15. Angular correlation function at $\rho=0.971$ (state a).

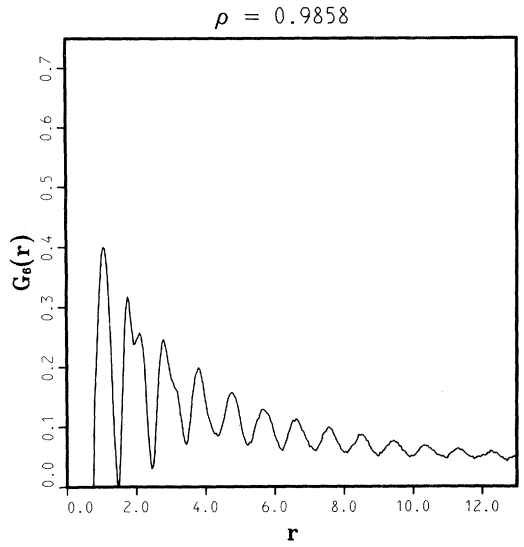

FIG. 16. Angular correlation function at $\rho = 0.986$ (state *b*).

large fluctuations in the grain structure. These requirements may not be satisfied for the system we studied here.

The value of the tail of $G_6(r)$ at $r = 13$ increases essentially monotonically as the density is increased toward the stable solid at state *f* with $\rho = 1.008$. This is consistent with the picture of a two-phase region with a nonzero solid fraction but finite-size effects make this conclusion less definite. In no case however could our data at densities less than 0.99 be fit assuming an algebraic decay with an exponent $\eta \leq 0.25$. Since it seems likely that errors due to small system size and finite run times would increase the apparent angular order, we believe this is good evidence that states with densities less than 0.986 are indeed ordinary fluids. We emphasize that in the two-phase region very long runs with equilibrium times of at least $48\,000\Delta t$ were necessary to reach these conclusions. Over shorter times large variations in $G_6(r)$ were found. This quantity, and the defect fraction F_D discussed before, show much larger fluctuations than the positional correlation function $g(r)$ or the thermodynamic properties.

X. VELOCITY AUTOCORRELATION FUNCTIONS AND DIFFUSION CONSTANTS

We have seen from $S(q)$, $G_6(r)$, and the Voronoi plots that the dense 2D fluid is highly ordered. Further evidence may be seen in the velocity autocorrelation functions of the crystal and fluid states. This function is defined as

$$\langle V(0)V(t)\rangle = \frac{1}{N}\sum_{i=1}^{N} V_i(0)V_i(t) \qquad (10.1)$$

where $V_i(0)$ is the velocity of particle *i* at some instant of time, and $V_i(t)$ is the velocity after an elapsed time *t*. This function normalized to unity at $t = 0$ is shown in Fig. 17 for states *f* and *b*. We note that at least three oscillations are observed for the stable solid in Fig. 17 before the function is essentially damped out. As would be expected the damping for the fluid is greater and only two oscillations are observed. This second oscillation is also observed for high-density 3D liquids but is *much* less pronounced, being present as a negative tail following the first minimum.[43]

The diffusion coefficient, proportional to zero-frequency value of the Fourier transform of the velocity autocorrelation function, is essentially zero for the solid but has finite value in the fluid. This behavior is more directly seen from plots of the mean-squared displacement ($\langle \Delta x^2 \rangle$) versus time, the limiting slope of which (ignoring long-wavelength fluctuations in this finite system) gives twice the diffusion coefficient. These are shown in Fig. 18 for states *f* and *b*. At a density of 0.971 the diffusion coefficient of the fluid is 0.038. It is interesting that this value is close to the diffusion coefficient for the 3D LJ fluid at its triple point, which has a value of 0.033.[44] The diffusion coefficient decreases rapidly as the fluid is compressed into the two-phase region, and at a density of 0.996 it is 0.011. This decreasing

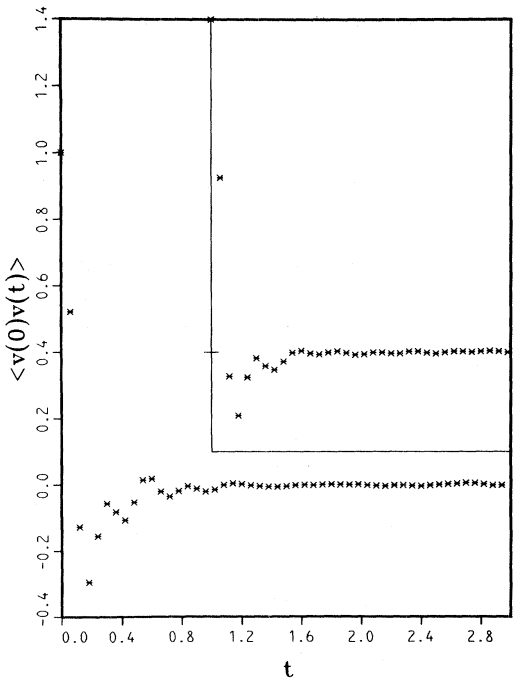

FIG. 17. Velocity autocorrelation function at $\rho = 1.008$ (state *f*), and $\rho = 0.986$ (state *b*). The insert represents the latter; both functions are to the same scale.

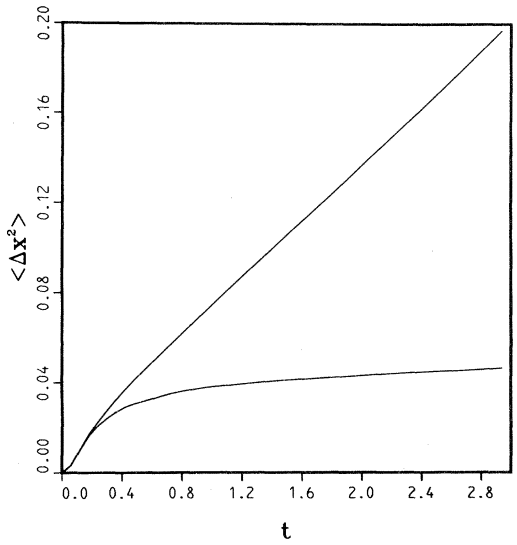

FIG. 18. Mean-squared displacement in x direction for $\rho = 1.008$ (state f) and for $\rho = 0.986$ (state b).

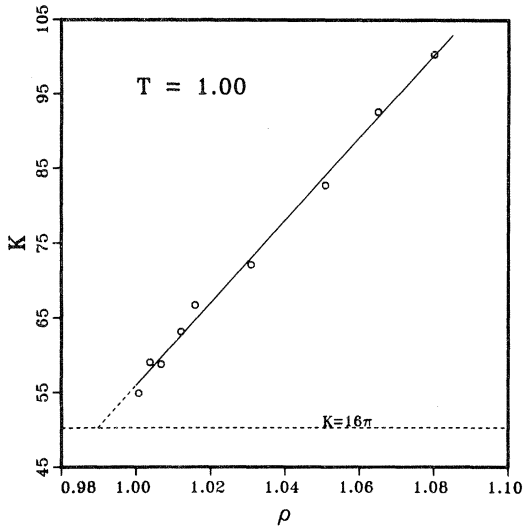

FIG. 19. Elastic constant ratio K [see Eq. (11.1)] vs density for the crystalline region of the $T = 1$ isotherm. The solid line represents the fit to the data given in Eq. (11.2).

mobility normally prevents the fluid from rearranging to form a perfect solid in an F traverse.

XI. ELASTIC CONSTANTS

One of the most important predictions of the HN theory[17] is that at the melting temperature a certain combination of elastic constants, K, takes on the universal value 16π. Here

$$K \equiv \frac{8}{\sqrt{3}} \left(\frac{\beta \mu^L}{\rho} \right) \Big/ \left(1 + \frac{\mu^L}{\mu^L + \lambda} \right) , \tag{11.1}$$

where μ^L and λ are the Lame (elastic) coefficients. The density and temperature dependence of the denominator is relatively small and the variation in K near melting is dominated by the behavior of $(\beta \mu^L / \rho)$. In Appendix C we discuss a new method for determining μ^L by the application of a finite shear to the system. Far from T_m we find that the statistical error in this determination of $(\beta \mu^L / \rho)$ is about 3%. Near T_m fluctuations are greater and the statistical error is as much as 5%.

Figure 19 shows the variation of K with density near melting along the $T = 1$ isotherm. Over this limited density region the data are fitted with an rms error of 1.12 by

$$K = -497.203 + 553.16\rho \ . \tag{11.2}$$

We find that at the melting density $\rho = 1.006$ determined earlier, $K = 59.3$, about 18% greater than 16π. This is consistent with the idea that a first-order transition intervenes before the KT instability takes place.

This value for K is fairly close to 16π, though the difference is outside our statistical error estimates. However, one could argue that our values for μ^L near melting are probably too large since we do not properly include the reduction in μ^L brought about by dislocation climb.

It is difficult to reach any firm conclusions as to the accuracy of our determination of K. Our present belief is that the small differences we see are meaningful but we are struck by the rather close agreement with the HN prediction for K at a melting transition that appears first order by every thermodynamic criterion. We must in some sense be close to the dislocation unbinding instability when the first-order transition takes place. A melting criterion based on Eq. (11.1) may be generally quite accurate. Workers studying other systems have also found good agreement with the HN melting criterion.[15,27]

XII. FINAL REMARKS

The thermodynamic data presented here seems to give a consistent description of the nature of phase transition for the r^{-12} system. The observation of a loop in the P-ρ isotherm and direct calculations of the free energy for the solid and fluid phases both suggest a conventional first-order transition. The location of the two-phase region and the coexistence pressure we find from both methods are in good agreement with each other. These thermodynamic data, which involve averages over fluctuations of all wavelengths, seem to be little affected by equilibration problems involving long-wavelength fluctuations.

In addition, trajectory plots of the elongated system showed the apparent coexistence of fluid and solid regions at a density corresponding to the center of the loop in the P-ρ isotherm. The fraction of fluid and solid remained essentially constant during a lengthy simulation, and the two phases persisted as singly-connected regions for long periods of time. However, very large fluctuations in the positions of the boundaries were observed, and this effect suggests a very small interface tension.

The change in the defect structure during the transition seems to be consistent with a first-order mechanism of melting with grain boundaries as the primary defect in the fluid.[19] Seldom are dislocations observed in the crystal, except in the form of opposite pairs separated by less than two atomic diameters. But the fluid contains linear arrays of dislocations that separate regions of fairly well-defined hexagonal order.

First-order melting is also suggested by significant changes in the properties of the system during the phase transition. A large increase in the mobility of the particles on melting is indicated both from the trajectory plots and measurements of the mean-squared displacements versus time. The Voronoi polyhedron analysis shows a large increase in the number of atoms that deviate from the sixfold coordination of the perfect crystal. In addition, the correlation functions exhibit significant changes during the transition.

We do observe large fluctuations in angular order and a rapid growth of correlations in the ordinary fluid phase as we approach the two-phase region identified by thermodynamic arguments. The fluid near freezing is certainly very well ordered by 3D standards as is made particularly evident in the structure factor $S(q)$. A system size larger than that we have used and still longer run times seem necessary to characterize the angular correlations in this fluid and to distinguish unequivocally between exponential decay with a large correlation length and power-law behavior. However, we doubt that a larger system size would have much effect on the thermodynamic properties, which appear quite stable and reproducible.

Thus the picture most consistent with all our data is that of a weak first-order transition which intervenes just before the solid becomes unstable to dislocation pair separation. The KT melting criterion predicts a melting density close to, but slightly below our estimate on the $T=1$ isotherm. The interface tension between the two phases is quite small, as indicated by the small amount of hysteresis found on entering the two-phase region on the $T=1$ isotherm from the fluid side.

The fluid region very near freezing displays some very interesting and unusual properties and deserves further investigation using a larger system size. There is still enough diffusion that we can reasonably hope to achieve equilibrium even for long-wavelength modes with a finite amount of computer time. Such a study would help resolve the remaining ambiguities in the characterization of angular correlations in the fluid caused by the system size we have used here.

ACKNOWLEDGMENTS

We are grateful to F. H. Stillinger and T. A. Weber for many helpful comments and have also profited from discussions with S. T. Chui, D. S. Fisher, B. I. Halperin, and D. R. Nelson.

APPENDIX A: SCALING AND THE HARMONIC SOLID

The temperature combines with the pair potential in the partition function for an inverse power system only in the combination

$$\beta u(r)=\beta\epsilon(\sigma/r)^n \ , \tag{A1}$$

where $\beta=(k_BT)^{-1}$ and the parameters σ and ϵ have dimensions of length and energy. We can eliminate the explicit temperature dependence by defining $\sigma_*=(\beta\epsilon)^{1/n}\sigma$ and rewriting Eq. (1) as $\beta u(r)=(\sigma_*/r)^n$. The dimensionless excess (over the ideal gas) thermodynamic properties then depend only on the single dimensionless state variable

$$\rho_*\equiv\rho\sigma_*^2=\rho\sigma^2(\beta\epsilon)^{2/n} \ . \tag{A2}$$

Systems with the same ρ_* have the same dimensionless excess thermodynamic properties and the melting or freezing curve is determined by the criterion $\rho_*\equiv$const. In particular the dimensionless excess Helmholtz free energy $\beta\Delta A/N$ is a function of ρ_* only. From the thermodynamic equations

$$\frac{\beta\Delta E}{N}=\beta\frac{\partial}{\partial\beta}\left[\frac{\beta\Delta A}{N}\right]_\rho \ , \tag{A3}$$

$$\frac{\beta\Delta P}{\rho}=\rho\frac{\partial}{\partial\rho}\left[\frac{\beta\Delta A}{N}\right]_\beta \ , \tag{A4}$$

it follows using Eq. (A2) that

$$\frac{\beta\Delta P}{\rho}=\frac{n}{2}\left[\frac{\beta\Delta E}{N}\right] \ . \tag{A5}$$

Other dimensionless thermodynamic properties can be related in a similar way. In what follows we specialize to $n=12$.

These scaling laws also apply to the harmonic solid since the reduced length σ_* can be introduced before the harmonic approximation is carried out. The ex-

cess (i.e., potential) energy of a harmonic system at a particular density has the form

$$\frac{\Delta E_H}{N} = \frac{\Delta E_0}{N} + kT \ , \tag{A6}$$

where E_0 is the energy at $T=0$. The dimensionless quantity $\beta \Delta E_H/N$ must be a function of ρ_* only and hence has the form

$$\frac{\beta \Delta E}{N} = c\rho_*^6 + 1 = \beta c \rho^6 + 1 \ , \tag{A7}$$

where c is the energy at $T=0$ and $\rho=1$. Evaluation of the lattice sum gives $c=1.267\,67$. The harmonic pressure is obtained immediately from Eq. (A5).

To obtain the chemical potential for the harmonic system we must also determine the free energy. Hence a calculation of the normal mode frequencies is required. The frequencies $w^2(\vec{k},s)$ for wave vector $\vec{k}$ and polarization $s(=1,2)$ are the eigenvalues of the 2×2 dynamical matrix $D_{ij}(\vec{k})$, which has been given in convenient computational form by Wallace[45] for central potentials and will not be reproduced here. The (classical) harmonic free energy is then given by

$$\beta A_H = \sum_{\vec{k},s} \ln[\beta \hbar w(\vec{k},s)] \ , \tag{A8}$$

where the sum is over wave vectors in the first zone and the two polarizations. The excess free energy is independent of $\hbar$ and the particle mass m as it should be in classical statistical mechanics since we subtract from Eq. (A8) the ideal gas free energy

$$\beta A_I/N = \ln(2\pi\beta\rho\hbar^2/m) - 1 \ . \tag{A9}$$

We have evaluated the harmonic free energy, Eq. (A8), using 780 and 3120 points in the first zone and found the differences where smaller than 10^{-3}. Scaling is also very accurately obeyed though not assumed in our program. From this we can determine the chemical potential, conveniently expressed in scaling form as

$$\beta \Delta \mu_H = \frac{\beta \Delta A_H}{N} + \frac{\beta \Delta P_H}{\rho}$$

$$= 9.9105 + 6\ln\rho_* + 8.873\,69\rho_*^6 \ . \tag{A10}$$

Wallace[45] also gives computationally convenient expressions for the $T=0$ elastic constants. Using these we find

$$\mu^L(T=0) = 15c\rho^7 = 19.015\rho^7 \ , \tag{A11}$$

$$\lambda(T=0) = 27c\rho^7 = 34.227\rho^7 \ . \tag{A12}$$

Finally the Einstein frequency, defined by

$$w_E^2 = \frac{1}{2N} \sum_{\vec{k},s} w^2(\vec{k},s) \tag{A13}$$

can also be simply determined. We find

$$w_E^2 = 157.91\rho^7 \ . \tag{A14}$$

APPENDIX B: ERRORS IN THE FREE-ENERGY ANALYSIS

In order to locate the coexisting densities ρ_l and ρ_s of the fluid and solid phases by thermodynamics we require equality of the pressure and chemical potential in the two phases. Here we determine the errors in the coexistence densities introduced by small errors in our determination of P and μ. If ρ_l and ρ_s are the exact fluid and solid coexistence densities we define

$$\delta P = P(\rho_l) - P(\rho_s) \ , \tag{B1}$$

$$\delta \mu = \mu(\rho_l) - \mu(\rho_s) \ , \tag{B2}$$

where $P(\rho)$ and $\mu(\rho)$ are our approximate expressions for the pressure and chemical potential. If we used the exact expressions for P and μ in Eqs. (B1) and (B2) then by definition δP and $\delta\mu$ vanish. To determine our apparent coexistence densities $\rho+\delta\rho$ we use our approximate expressions and satisfy instead

$$P(\rho_l + \delta\rho_l) = P(\rho_s + \delta_s) \ , \tag{B3}$$

$$\mu(\rho_l + \delta\rho_l) = \mu(\rho_s + \delta\rho_s) \ . \tag{B4}$$

We assume $\delta\rho \ll \rho$ and find to lowest order

$$P(\rho_l) + K_l\delta\rho_l = P(\rho_s) + K_s\delta\rho_s \ , \tag{B5}$$

$$\mu(\rho_l) + K_l\frac{\delta\rho_l}{\rho_l} = \mu(\rho_s) + K_s\frac{\delta\rho_s}{\rho_s} \ , \tag{B6}$$

where $K \equiv (\partial P/\partial\rho)_T$ and we have used the thermodynamic identity $(\partial\mu/\partial\rho)_T = (1/\rho)(\partial P/\partial\rho)_T$. Using Eqs. (B1) and (B2) and solving Eqs. (B5) and (B6) for $\delta\rho_l$ and $\delta\rho_s$ we find

$$\left(\frac{\delta\rho_s}{\rho_s}\right) = \frac{\delta P - (\delta\mu)\rho_l}{K_s(\rho_s - \rho_l)} \ , \tag{B7}$$

$$\left(\frac{\delta\rho_l}{\rho_l}\right) = \frac{\delta P - (\delta\mu)\rho_s}{K_l(\rho_s - \rho_l)} \ . \tag{B8}$$

For the r^{-12} system we have $K_s \cong 50$ and $\rho_s - \rho_l \cong 0.02$ so the denominators in Eq. (B7) and (B8) are near unity.

Equations (B7) and (B8) show we must determine P and μ accurately if we want an accurate location of the melting and freezing densities. The situation becomes much worse for potentials r^{-n} with smaller values of n where the change in density is even smaller. Indeed this change must tend to zero as $n \to 2$, even if the transition remains first order.[37]

However, we determine μ from integration of the pressure. If there are systematic errors in P then δP and $\delta\mu$ will be of the same sign and the final error in $\delta\rho$ from Eqs. (B7) and (B8) will not be as large as might have been expected. For example, as argued in this paper, let us assume that the fluid branch of the $T=1$ isotherm has been determined accurately, but that as we approach the melting density on the solid branch the pressure is systematically low because of difficulties in obtaining the proper number of defects. To get an order of magnitude estimate assume that for densities smaller than some ρ_1, K_s differs from the correct value by an amount δK. Then $\delta P \cong \delta K(\rho_s-\rho_1)$ and $\delta\mu \cong \delta K(\rho_s-\rho_1)/\rho_1$. Thus, from Eq. (B7), assuming the denominator is unity,

$$\left(\frac{\delta\rho_s}{\rho_s}\right) \cong \delta P\left(1-\frac{\rho_l}{\rho_1}\right) . \tag{B9}$$

A conservative estimate for ρ_1 is 1.08; this corresponds by scaling to a temperature $T=0.63T_m$ at $\rho=1$ and it is hard to believe an incorrect treatment of defects could make significant contributions to the pressure at temperatures lower than this. Thus the error in $\delta\rho/\rho_s$ from Eq. (B9) is only about 0.1 of the error in δP at melting.

APPENDIX C: CALCULATION OF ELASTIC CONSTANTS

Squire *et al.*[46] have derived expressions for the elastic constants by considering the change in free energy arising from an infinitesinal change in shape of the crystal. The resulting equations contain fluctuation terms and the final result is expressed as the difference of two rather large and fluctuating quantities. Similar difficulties arise when considering the usual fluctuation formula for the specific heat. In the latter case more accurate results can often be obtained by calculating the energy for a series of nearby temperatures and numerically differentiating the result. We decided to apply a similar approach to the determination of the elastic constants. These can be determined from the linear terms relating the variation of the stress (pressure) tensor to a given finite strain. This method has the advantage of avoiding the fluctuation terms and also allows us to study such interesting questions as shear induced dislocation motion. On the other hand there is the danger of a very nonlinear response (plastic flow) in the strained crystal, particularly near the melting transition. However it is easy to determine from the data if plastic flow has occurred. We found for the r^{-12} system that as long as we limited ourselves to small strain (2% or less) we were not troubled by plastic flow even very near the melting transition.

One should note that the unstrained repulsive force system is not at zero pressure as is assumed in many textbooks.[47] Thus the relation between the effective Lamé coefficients λ and μ^L used in the HN theory and the usual elastic constants C_{ijkl} contains extra terms involving the pressure. This point has been discussed in detail by Stewart[48] and by Wallace[45] and should not be forgotten when using the method of Squire *et al.*[46]

In our method we obtain the shear modulus μ^L directly by considering the stress tensor in a system with modified boundary conditions and a given (shear) strain. Thus if R_x and R_y are the x and y coordinates of a particle in an equilibrated unstrained state we apply a coordinate transformation $(R_x,R_y)\rightarrow(r_x,r_y)$ where

$$r_x=R_x+u_{xy}R_y , \quad r_y=R_y . \tag{C1}$$

This produces a system with uniform shear measured by u_{xy} and the same area as the original system. The periodic boundary conditions, originally of the form

$$(R_x+L_x,R_y+L_y)\rightarrow(R_x,R_y) \tag{C2}$$

where L_x and L_y are the lengths of the rectangular periodic box in the x and y directions, are now modified to accomodate a system with uniform shear:

$$(r_x+u_{xy}L_y,r_y+L_y)\rightarrow(r_x,r_y) . \tag{C3}$$

The resulting stress under the given strain u_{xy} can be determined from the (x,y) component of the stress (pressure) tensor $P_{xy}(u_{xy})$ (Ref. 49)

$$\frac{\beta P_{xy}(u_{xy})}{\rho}=\frac{1}{N}\sum_{i<j}^{N}\left\langle\beta u'(r_{ij})\frac{(x_i-x_j)(y_i-y_j)}{r_{ij}}\right\rangle_{u_{xy}} , \tag{C4}$$

where $\langle\ \rangle_{u_{xy}}$ is a normalized ensemble average in the modified system with the given strain u_{xy}. The Lamé coefficient (shear modulus) μ^L is then determined from the linear term in the stress-strain relation

$$P_{xy}(u_{xy})=\mu^L u_{xy}+O(u_{xy}^2) . \tag{C5}$$

We find the statistical errors in our determination of μ^L to be about 3% at a state about half the melting temperature. We observe somewhat larger fluctuations near T_m but have made much longer runs there also. If plastic flow has occurred there will be a sudden drop in μ^L during the course of the MD run. Using values of u_{xy} of 2% or less we saw no evidence for plastic flow even at the melting density $\rho=1.006$.

To test the HN prediction in Eq. (11.1) we must also obtain the combination $\lambda+u^L$. It is simplest to obtain this assuming that the bulk modulus satisfies .

$$\rho\left(\frac{\partial P}{\partial\rho}\right)_\beta=\lambda+\mu^L . \tag{C6}$$

Actually there are corrections due to vacancies and interstitials which in principle cause Eq. (C6) to be slightly inaccurate at finite temperatures,[50] but these should be very small for our system. Furthermore the KT criterion depends much more critically on determining an accurate value for μ^L near melting than it does on $\lambda + \mu^L$. We believe the errors entailed from the use of Eq. (C6) are small compared to the inherent errors in determining μ^L as described above.

[1]For a recent general review see D. R. Nelson, in *Proceedings of the 1980 Summer School on Fundamental Problems in Statistical Mechanics* (Enschede, The Netherlands, in press).

[2]See, e.g., R. J. Birgeneau, E. M. Hammonds, P. Heiney, and P. W. Stephens, in *Ordering in Two Dimensions,* edited by S. K. Sinha (North-Holland, Amsterdam, 1980), p. 29 and references therein.

[3]C. C. Grimes and G. Adams, Phys. Rev. Lett. 42, 795(1979).

[4]P. Pieranski, Phys. Rev. Lett. 45, 569 (1980).

[5]See, e.g., R. Pindac, D. E. Moncton, S. C. Davey, and J. W. Goodby, Phys. Rev. Lett. 46, 1134 (1981).

[6]P. R. Couchman and W. A. Jesser, Philos. Mag. 35, 787 (1977). For a simulation study that suggests layer melting see J. Q. Broughton and L. V. Woodcock, J. Phys. C 11, 2743 (1978).

[7]B. J. Alder and T. E. Wainright, Phys. Rev. 127, 59 (1962); W. W. Wood, in *Physics of Simple Liquids,* edited by H. N. V. Temperley, J. S. Rowlinson, and G. S. Rushbrooke (North-Holland, Amsterdam, 1968), p. 115.

[8]R. M. J. Cotterill and L. B. Pedersen, Solid State Commun. 10, 439 (1972); T. Tsien and J. P. Valleau, Mol. Phys. 27, 177 (1974); S. Toxvaerd, J. Chem. Phys. 69, 4750 (1978).

[9]See, e.g., W. G. Hoover and M. Ross, Contemp. Phys. 12, 339 (1971) for a review of some of these ideas. See also H. C. Longuett-Higgins and B. Widom, Mol. Phys. 8, 549 (1964).

[10]R. E. Peierls, Ann. Inst. Henri Poincaré 5, 177 (1935).

[11]L. Landau, Phys. Z. Sowjetunion II, 26 (1937).

[12]D. A. Young and B. J. Alder, J. Chem. Phys. 60, 1254 (1974).

[13]R. C. Gann, S. Chakravarty, and G. V. Chester, Phys. Rev. B 20, 326 (1979).

[14]There are power-law divergences as k approaches a reciprocal-lattice vector rather than the δ-function behavior found in 3D systems. See B. Jancovici, Phys. Rev. Lett. 19, 20 (1967).

[15]J. Tobochnick and G. V. Chester (unpublished).

[16]J. M. Kosterlitz and D. J. Thouless, J. Phys. C 6, 1181 (1973); J. M. Kosterlitz, *ibid.* 7, 1046 (1974).

[17]B. I. Halperin and D. R. Nelson, Phys. Rev. Lett. 41, 121 (1978); D. R. Nelson and B. I. Halperin, Phys. Rev. B 19, 2457 (1979).

[18]A. P. Young, Phys. Rev. B 19, 1855 (1979).

[19]S. T. Chui (unpublished).

[20]D. Frenkel and J. P. McTague, Phys. Rev. Lett. 42, 1632 (1979).

[21]J. Tobochnick and G. V. Chester, in *Ordering in Two Dimensions,* edited by S. K. Sinha (North-Holland, Amsterdam, 1980), p. 339

[22]F. F. Abraham, Phys. Rev. Lett. 44, 463 (1980); in *Ordering in Two Dimensions,* edited by S. K. Sinha (North-Holland, Amsterdam, 1980), p. 155; and (unpublished).

[23]J. A. Barker, D. Henderson, and F. F. Abraham, Physica (Utrecht) 106A, 226 (1981).

[24]S. Toxvaerd, Phys. Rev. Lett. 44, 1002 (1980).

[25]F. van Swol, L. V. Woodcock and J. N. Cape, J. Chem. Phys. 73, 913 (1980).

[26]F. H. Stillinger and T. A. Weber, J. Chem. Phys. 74, 4015 (1981); T. A. Weber and F. H. Stillinger, *ibid.* 74, 4020 (1981).

[27](a) R. Morf, Phys. Rev. Lett. 43, 931 (1979). (b) R. K. Kalia, P. Vashishta, and S. W. de Leeuw, Phys. Rev. B 23, 4794 (1981); R. K. Kalia and P. Vashishta, J. Phys. C 14, L642 (1981).

[28]J. P. McTague, D. Frenkel, and M. P. Allen, in *Ordering in Two Dimensions,* edited by S. K. Sinha (North-Holland, Amsterdam, 1980), p. 147; and (unpublished).

[29]D. S. Fisher, B. I. Halperin, and R. Morf, Phys. Rev. B 20, 4692 (1979).

[30]Some of these problems have been discussed by D. P. Landau and K. Binder, Phys. Rev. B 17, 2328 (1978).

[31]H. J. Leamy, G. H. Gilmer, and K. A. Jackson, in *Surface Physics of Materials* (Academic, New York, 1975), Vol. 1, p. 121; R. Swendsen, Phys. Rev. B 15, 5421 (1977); 18, 492 (1978); W. J. Shugard, J. D. Weeks, and G. H. Gilmer, Phys. Rev. Lett. 41, 1399 (1978); J. Tobochnick and G. V. Chester, Phys. Rev. B 20, 3761 (1979).

[32]W. G. Hoover, S. G. Gray, and K. W. Johnson, J. Chem. Phys. 55, 1128 (1971).

[33]For more details about the MD procedure see J. Q. Broughton, G. H. Gilmer, and J. D. Weeks, J. Chem. Phys. 75, 5128 (1981).

[34]J. E. Mayer and W. W. Wood, J. Chem. Phys. 42, 4268 (1965).

[35]Van Swol *et al.* (Ref. 25) used Ross's melting law to estimate from their data a first-order transition with $P_m = 12.5$, $\rho_l = 0.95$, and $\rho_s = 0.97$.

[36]This procedure was used in Ref. 13 for the $n = 1$ system and in Ref. 23 for the LJ system.

[37]J. D. Weeks, Phys. Rev. B 24, 1530 (1981).

[38]R. Collins, in *Phase Transitions and Critical Phenomena,* edited by C. Domb and M. S. Green (Academic, New York, 1972), Vol. 2, p. 271.

[39]We are grateful to T. A. Weber for providing us with his computer program which performs the Voronoi analysis.

[40]J. P. Hansen and L. Verlet, Phys. Rev. 184, 150 (1969).

[41]T. V. Ramakrishnan and M. Yussouff, Phys. Rev. B 19, 2775 (1979).

[42]This definition is the same as used by J. A. Zollweg, in *Ordering in Two Dimensions,* edited by S. K. Sinha (North-Holland, Amsterdam, 1980), p. 331. Frenkel and McTague's definition (Ref. 20) sets $n = 6$ for each particle but this difference is probably unimportant.

[43]J. Krishick and B. J. Berne, J. Chem. Phys. 59, 3732 (1973).

[44]See, e.g. J. Q. Broughton, A. Bonissent, and F. F. Abraham, J. Chem. Phys. 74, 4029 (1981).
[45]D. J. Wallace, *Thermodynamics of Crystals* (Wiley, New York, 1972).
[46]D. R. Squire, A. C. Holt, and W. G. Hoover, Physica (Utrecht) 42, 388 (1968).
[47]This is assumed, for example, in L. Landau and E. M. Lifshitz, *Theory of Elasticity* (Pergamon, New York, 1970).
[48]G. A. Stewart, Phys. Rev. A 10, 671 (1974).
[49]J. H. Irving and J. G. Kirkwood, J. Chem. Phys. 18, 817 (1950).
[50]A. Zippelius, B. I. Halperin, and D. R. Nelson, Phys. Rev. B 22, 2514 (1980).